# Climatic versus biotic constraints on carbon and water fluxes in seasonally drought-affected ponderosa pine ecosystems

# Climatic versus biotic constraints on carbon and water fluxes in seasonally drought-affected ponderosa pine ecosystems

P. A. Schwarz,[1] B. E. Law,[1] M. Williams,[2] J. Irvine,[1] M. Kurpius,[3] and D. Moore[1]

Received 5 February 2004; revised 28 June 2004; accepted 26 July 2004; published 15 October 2004.

[1] We investigated the relative importance of climatic versus biotic controls on gross primary production (GPP) and water vapor fluxes in seasonally drought-affected ponderosa pine forests. The study was conducted in young (YS), mature (MS), and old stands (OS) over 4 years at the AmeriFlux Metolius sites. Model simulations showed that interannual variation of GPP did not follow the same trends as precipitation, and effects of climatic variation were smallest at the OS (<10%), largest at the MS (>50%), and intermediate at the YS (<20%). In the young, developing stand, interannual variation in leaf area has larger effects on fluxes than climate, although leaf area is a function of climate in that climate can interact with age-related shifts in carbon allocation and affect whole-tree hydraulic conductance. Older forests, with well-established root systems, appear to be better buffered from effects of seasonal drought and interannual climatic variation. Interannual variation of net ecosystem exchange (NEE) was also lowest at the OS, where NEE is controlled more by interannual variation of ecosystem respiration, 70% of which is from soil, than by the variation of GPP, whereas variation in GPP is the primary reason for interannual changes in NEE at the YS and MS. Across spatially heterogeneous landscapes with high frequency of younger stands resulting from natural and anthropogenic disturbances, interannual climatic variation and change in leaf area are likely to result in large interannual variation in GPP and NEE. *INDEX TERMS:* 0315 Atmospheric Composition and Structure: Biosphere/atmosphere interactions; 1615 Global Change: Biogeochemical processes (4805); 1851 Hydrology: Plant ecology; 3210 Mathematical Geophysics: Modeling; *KEYWORDS:* gross primary production, net ecosystem $CO_2$ exchange, interannual variation, climatic variation, drought, ponderosa pine

**Citation:** Schwarz, P. A., B. E. Law, M. Williams, J. Irvine, M. Kurpius, and D. Moore (2004), Climatic versus biotic constraints on carbon and water fluxes in seasonally drought-affected ponderosa pine ecosystems, *Global Biogeochem. Cycles*, *18*, GB4007, doi:10.1029/2004GB002234.

## 1. Introduction

[2] Temperate forests are an important component of the terrestrial carbon cycle, and it is generally believed that these forests are net sinks for atmospheric carbon [*Myneni et al.*, 2001; *Goodale et al.*, 2002]. Both climate [e.g., *Schimel et al.*, 2000, 2001; *Schaefer et al.*, 2002] and time since stand-replacing disturbance [e.g., *Turner et al.*, 1995; *Caspersen et al.*, 2000; *Law et al.*, 2001b, 2003] have been identified as important controls on the net ecosystem exchange of $CO_2$. Even within a single forest type, disturbances such as wildfire and timber harvesting have resulted in spatially heterogeneous landscapes in the western United States [*Cohen et al.*, 1996]. Consequently, many western landscapes are mosaics of forest stands in different stages of development (Figure 1) with a range of carbon stocks and fluxes [*Law et al.*, 2003, 2004].

[3] Detailed, process-based simulation models provide an approach for integrating knowledge of ecophysiological processes and scaling these processes to stand and ecosystem levels [*Landsberg and Gower*, 1997; *Ryan*, 2002]. Previously, we evaluated the detailed process model, Soil-Plant-Atmosphere (SPA), in an old-growth ponderosa pine forest (*Pinus ponderosa* var. ponderosa) in Central Oregon, using eddy covariance estimates of whole ecosystem gross photosynthesis (GPP) and water vapor exchange [*Law et al.*, 2000], and made subsequent modifications of the model treatment of root access to soil water [*Williams et al.*, 2001b].

[4] In this study, we took advantage of a unique collection of data collected at AmeriFlux sites in young (YS) 20-, mature (MS) 90-, and old (OS) >200-year-old stands of ponderosa pine in the Metolius River area in central Oregon (Figure 1). At these sites, in addition to stand-level data on $CO_2$ and water vapor exchange, the structure, physiological

[1]College of Forestry, Oregon State University, Corvallis, Oregon, USA.
[2]School of GeoSciences, University of Edinburgh, Edinburgh, UK.
[3]College of Oceanic and Atmospheric Sciences, Oregon State University, Corvallis, Oregon, USA.


0886-6236/04/2004GB002234

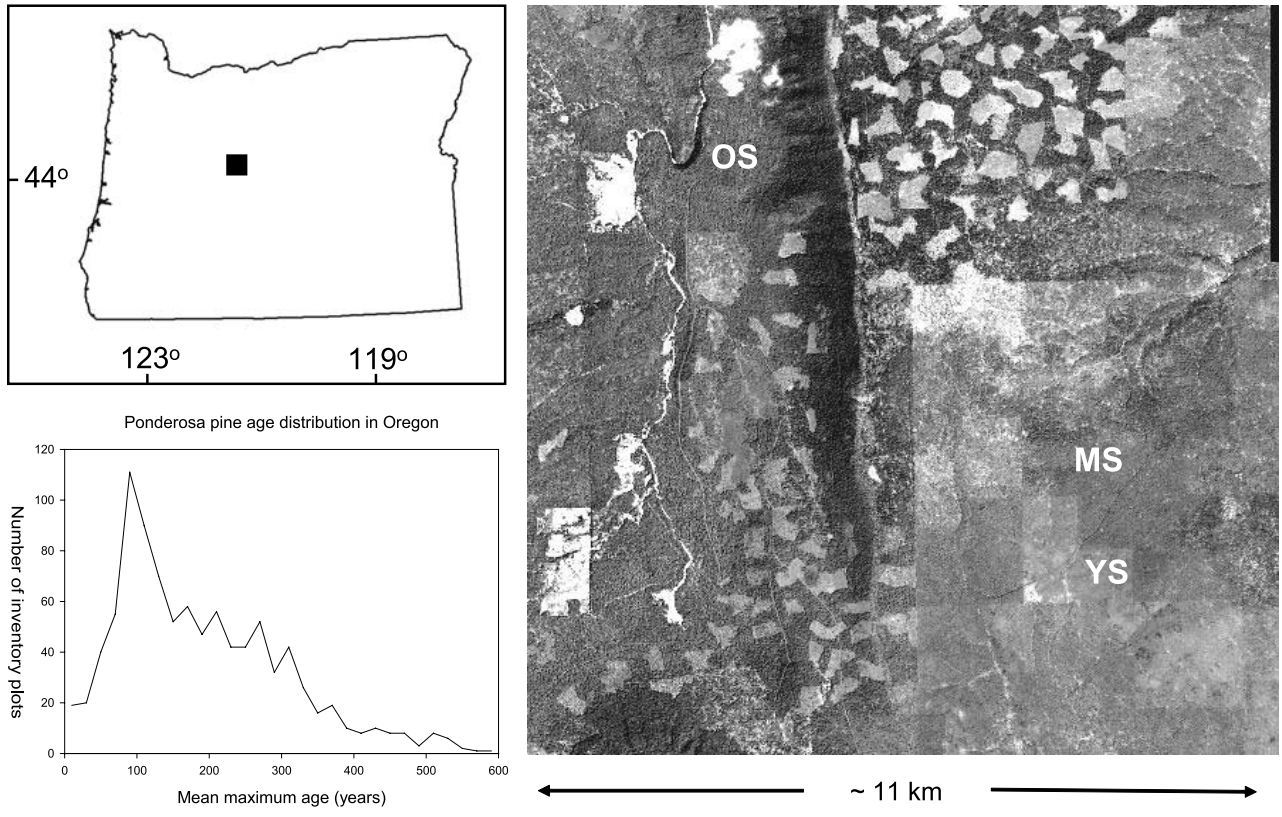


**Figure 1.** IKONOS image of the Metolius River area of central Oregon showing the locations of the young site (YS), mature site (MS), and old site (OS) and the spatial heterogeneity of stand structure and development stages. The distribution of stand ages is shown in the lower left.

characteristics, and soil properties were measured to explain variation in ecosystem fluxes in this semi-arid region subject to summer drought.

[5] The goal of this study was to investigate systematically the relative importance of climatic versus biotic controls on GPP and water vapor exchange over a 4-year period. Our objectives were (1) to parameterize the SPA model for three ponderosa pine stands with differing age structure and stand characteristics but otherwise growing under similar climate and environmental conditions and then to compare, for each of the three stands, simulated and field-measured estimates of tree transpiration, total latent energy (LE) fluxes, and GPP derived from eddy covariance data; (2) to carry out a sequence of simulations designed to evaluate the potential relative importance of climate, climatic variation over 4 years, and stand-related biotic factors such as leaf area and hydraulic conductance as controls on interannual variation of GPP; and (3) to examine the implications of interannual variation of GPP and ecosystem respiration on net ecosystem exchange of $CO_2$ (NEE). This is the first time we have used such a large amount of site-specific data to parameterize the SPA model for different age stands and for several years of different climate. We hypothesized that interannual variation of GPP at these sites was controlled primarily by climatic factors, such as precipitation, but that the magnitude of the interannual variation was determined by site-specific biotic factors.

## 2. Methods

### 2.1. Study Sites

[6] The three sites selected for this study are in the eastern Cascade Mountains near Sisters, Oregon, and are located within 8 km of one another. The Metolius sites are part of the AmeriFlux network [*Hargrove et al.*, 2003]. All three sites have an exclusive overstory of ponderosa pine trees but

**Table 1.** Selected Site and Stand Characteristics for the Young Site (YS), Mature Site (MS), and Old Site (OS), Which are Located in the Metolius Area of Central Oregon

| | YS | MS | OS |
|---|---|---|---|
| Latitude | 44.437 | 44.451 | 44.498 |
| Longitude | −121.568 | −121.558 | −121.625 |
| Elevation, m | 1165 | 1232 | 895 |
| Mean tree height, m | 4.3 | 14.0 | 38.9 |
| Stand age, years | 23 | 89 | 190 |
| Foliar nitrogen, g $m^{-2}$ | 2.1–2.9 | 2.1–2.9 | 2.0–3.6 |
| Sand, % | 54–69 | 59–67 | 63–67 |
| Clay, % | 5–11 | 8–11 | 10–11 |
| Soil organic matter, % | 2.2 | 3.0 | 3.0 |
| Soil porosity, % | 54–59 | 53–61 | 54–61 |

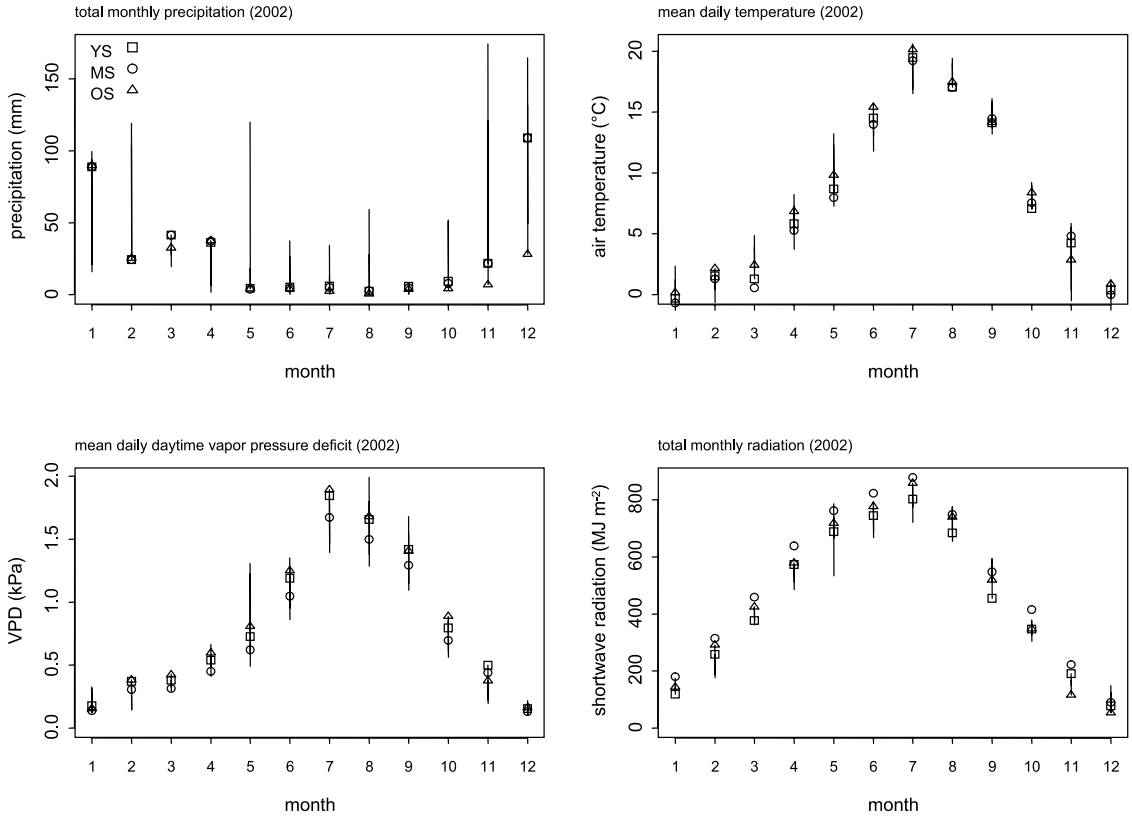


**Figure 2.** Monthly climate data for each site during 2002 showing seasonal trends. Vertical bars show the range of variation in the monthly values during the 4 years of the study, 1999–2002.

differ in their age structure and understory composition (Table 1). The young pine site (YS) was clear-cut in 1978 and then allowed to regenerate naturally, and understory shrubs account for approximately 40% of the site's leaf area index [*Law et al.*, 2001a]. The mature site (MS) was also clear-cut and allowed to regenerate naturally, and the average tree age is now about 90 years. The old-growth site (OS) site has never been logged and consists of old (250 years), young (60–70 years), and mixed-age patches of ponderosa pine. All three sites are nearly level, with sandy, well-drained soils with relatively little organic matter and little evidence of surface runoff (Table 1). Details regarding site conditions and soils are described by *Law et al.* [2001c, 2003].

### 2.2. Climatic Characteristics

[7] The three sites have similar climate typical of the semi-arid region of central Oregon: warm, dry summers and cool, wet winters. Four years of meteorological data (1999–2002) were available for the YS and OS, whereas only 1 year of data (2002) was available for the MS. The YS and MS are about 2 km apart and several hundred meters higher in elevation than the OS and are ~0.5–1.0 degrees cooler (Figure 2). At the sites, annual precipitation varies between 300 and 600 mm, with the majority falling between November and April as both rain and snow. The winter snowpack generally sustains these forests through summer drought, and rain on snow events can increase runoff to streams, limiting summer water availability to trees. During the 4 years of the study, mid-summer rainfall (June 1 to September 30) accounted for less than 15% of total annual precipitation. The 30-year mean annual precipitation, based on data from the Sisters Ranger Station (~15 km east of the study sites), is 360 mm $yr^{-1}$. Although precipitation patterns are highly variable from year to year, they are generally synchronous among the three sites. Other meteorological conditions are similar among the three sites and have substantially less interannual variation than precipitation.

### 2.3. Environmental Measurements

[8] In 2002, rates of soil water depletion across different soil horizons were estimated from calibrated, periodic time domain reflectometry (TDR) measurements in three soil pits at each site. Continuous environmental measurements at each site included meteorological conditions as well as eddy flux measurements of net carbon exchange ($F_c$) and whole-ecosystem water fluxes. Meteorological and micrometeorological instruments were installed at a height of 47 m at the OS (14 m above the forest canopy), 31 m at the MS (15 m above the canopy), and 12 m at the YS (9 m above the canopy). Meteorological variables measured at each site

consisted of half-hour means calculated from measurements at the top of the instrument tower at each of the sites and included air temperature, vapor pressure deficit, wind speed and direction, global shortwave solar radiation, photosynthetically active radiation (PAR), net radiation, and precipitation. After data screening and gap filling, these data were used to drive the SPA model.

[9] NEE and total LE fluxes were computed from the micrometeorological data using the eddy covariance technique. At the YS, eddy covariance measurements have been made continuously since the beginning of April 2000 [*Anthoni et al.*, 2002], and similar measurements have been made at the OS from 1996 until the instruments were moved to the MS at the end of 2001 [*Anthoni et al.*, 1999; *Law et al.*, 1999a, 1999b]. Full details of the instrumentation and sampling methodology for the OS and YS are described by *Anthoni et al.* [2002] and by M. R. Kurpius et al. (Annual carbon exchange along a ponderosa pine chronosequence, submitted to *Journal of Geophysical Research*, 2004) (hereinafter referred to as Kurpius et al., submitted manuscript, 2004) for the MS. All flux data were summarized and stored at half-hour intervals, screened, and filtered based on a friction velocity threshold for wind speed (described below) prior to being made available for further analysis [*Anthoni et al.*, 2002]. Data collected on rainy days were excluded from the final data set for comparison with the SPA model because of the effects of rain droplets on the sonic anemometers and open-path infrared gas analyzers.

[10] Flux-based estimates of gross primary production (GPP) were calculated as the sum of NEE and ecosystem respiration ($R_e$), the latter of which was calculated from nighttime net carbon exchange from the eddy covariance system and an empirical, Arrhenius-type function of temperature [*Anthoni et al.*, 2002]. The parameters of the function were estimated seasonally and thus implicitly accounted for gross changes in soil moisture. On the basis of examination of $F_c$ versus $\underline{u}^*$ at night and comparison of $R_e$ calculated from nighttime $F_c$ ($R_{e.ec}$) versus $R_e$, calculated from summed soil, foliage, and sapwood respiration fluxes ($R_s + R_f + R_w$), we determined that local topography affects $F_c$ under conditions of low turbulence at all three sites. We found a dependence of $F_c$ on $u^*$ when $u^* < 0.2$ m s$^{-1}$ at YS and OS and $u^* < 0.35$ m s$^{-1}$ at MS. Following the removal of $F_c$ data below the $u^*$ threshold and subsequent gap filling using the regression method outlined by *Falge et al.* [2001], we achieved good agreement between $R_{e.ec}$ and $R_s + R_f + R_w$ [*Anthoni et al.*, 2002, Kurpius et al., submitted manuscript, 2004]. Additional research is being conducted to further understand the role of local topography on nighttime $F_c$.

### 2.4. Structural and Physiological Measurements

[11] Leaf area index (LAI) was estimated at the YS and OS in 1999, 2001, and 2002, and at the MS in 2001 and 2002 using the optical approach described by *Law et al.* [2001a]. At each site, light transmittance was measured at 39 predetermined locations using an LAI-2000 Plant Canopy Analyzer (Li-Cor, Inc., Lincoln, Nebraska). Mean LAI was calculated and then corrected for wood interception and for clumping of shoots and needles within shoots according to methods outlined by *Law et al.* [2001a]. In 2002, LAI was measured in early spring, prior to the expansion of current year needles, and again in late summer during maximum seasonal leaf area to estimate the seasonal changes in leaf area. In 1999 and 2001, LAI was measured at the seasonal maximum. Examination of the measurements of maximum seasonal LAI suggested that leaf area at the YS was increasing by about 17% per year over the 4-year period, whereas maximum seasonal leaf area at the OS and MS were essentially constant.

[12] Fine root biomass (live roots $\leq$2 mm diameter) was measured in 2002 to a depth of 1 m by extracting soil cores at 18 locations within each site [*Law et al.*, 2003; *Sun et al.*, 2004]. In the laboratory, roots from the cores were sorted into live and dead fractions according to size class. These data were used to estimate surface root density ($F_{max}$), total root biomass ($F_{total}$), and rooting depth ($D_{max}$), all required parameters for the model (described below).

[13] Tree transpiration was estimated by measuring sap flux density continuously between April and November at each site using a heat dissipation technique [*Granier*, 1987]. Three years of data (2000–2002) were available for the OS and YS and one full year of data (2002) was available for the MS. Site-level estimates of tree transpiration were calculated by scaling the sap flux measurements using sapwood area relationships and stand density information. Details regarding the methodology and site-level scaling of tree transpiration are provided by *Irvine et al.* [2002].

[14] Net assimilation ($A-C_i$ curves with an LI-6400; LICOR, Lincoln, Nebraska) and foliar nitrogen were measured seasonally on shoots from trees and on shrubs. Predawn leaf water potential was also measured seasonally, and midday water potentials were made in mid-summer to estimate the critical water potential threshold required by the model.

### 2.5. SPA Model

[15] The soil-plant-atmosphere (SPA) model is a process model that simulates ecosystem photosynthesis, energy balance, and water transport. The model was designed for direct comparisons with eddy covariance estimates of carbon and water fluxes and has been successfully implemented in temperate [*Williams et al.*, 1996, 2001b], tropical [*Williams et al.*, 1998], and arctic ecosystems [*Williams et al.*, 2000]. The model uses 10 canopy layers to partition vertical structure of the forest canopy and uses a detailed radiative transfer scheme that calculates sunlit and shaded fractions of the foliage in each layer [*Williams et al.*, 2001b]. The model also has 20 soil layers into which fine root biomass is distributed that are used to simulate the transfer and uptake of soil water received from precipitation events. Detailed descriptions of the fundamental equations, model logic, algorithms, and the development history of the SPA model are given by *Williams et al.* [1996, 2001b].

### 2.6. Model Parameterization and Calibration

[16] For each site, measured net assimilation in relation to leaf internal $CO_2$ concentrations were used to derive estimates of maximum carboxylation ($V_{cmax}$) and electron transport ($J_{max}$) rates [*Farquhar and von Caemmerer*, 1982], which are required parameters of the model (Table 2). The

**Table 2.** Key Parameter Values for the Soil-Plant-Atmosphere (SPA) Model Determined From Structural and Physiological Measurements at Each of the Study Sites

| Parameter Description | Units | YS | MS | OS |
|---|---|---|---|---|
| Critical leaf water potential prior to cavitation | MPa | −1.7 | −1.7 | −1.7 |
| Daily foliar nitrogen concentration | g N $m^{-2}$ | 2.1–2.9 | 2.1–2.9 | 1.95–3.6 |
| Maximum carboxylation capacity ($V_{cmax}$) | μmol $m^{-2}$ $s^{-1}$ | 48.9 | 48.9 | 48.9 |
| Maximum electron transport rate ($J_{max}$) | μmol $m^{-2}$ $s^{-1}$ | 131.6 | 131.6 | 131.6 |
| $V_{cmax}$ per unit leaf nitrogen | μmol g $N^{-1}$ $s^{-1}$ | 17.5 | 19.6 | 14.4 |
| $J_{max}$ per unit leaf nitrogen | μmol g $N^{-1}$ $s^{-1}$ | 47.0 | 52.6 | 38.7 |
| Daily leaf area index (LAI) in 2002 | $m^2$ $m^{-2a}$ | 0.86–1.46 | 2.77–3.44 | 2.19–2.74 |
| Stem-specific hydraulic conductivity | mmol $m^{-1}$ $s^{-1}$ $MPa^{-1}$ | 14 | 6 | 10 |
| Root resistivity | MPa s g $mmol^{-1}$ | 12 | 3 | 10 |
| Rooting depth | m | 0.9–1.0 | 1.1 | 1.8 |
| Maximum root biomass per unit volume ($F_{max}$) | g $m^{-3}$ | 3800 | 1500 | 1400 |
| Total fine root biomass ($F_{total}$), min–max | g $m^{-2}$ | 450–650 | 715 | 400 |

[a]Denotes $m^2$ half-surface area of foliage per $m^2$ ground.

two optical estimates of LAI during 2002 and measurements of foliar nitrogen along with observations of seasonal phenology (bud break, needle elongation, and senescence) at the sites were used to derive, via linear interpolation, daily estimates of LAI and foliar nitrogen for both the understory and the trees. Understory leaf area was assigned to the lowest canopy layer of the model, and the leaf area of the trees was distributed among the upper canopy layers. For the YS, additional years of daily LAI and foliar nitrogen were prepared in accordance with the observed rate of increase of LAI at the site.

[17] Using field measurements of fine root biomass ($F_{total}$) in the top meter of soil, we estimated numerically the parameters ($F_{max}$, $D_{max}$) of the exponential function that describes the vertical distribution of roots in the model [*Williams et al.*, 2001b]. The model also uses depth-specific estimates of soil texture to calculate the soil hydraulic conductivity and the energy balance at the soil surface. These data were available from previous studies for YS and OS [*Law et al.*, 2001c] and for the MS [*Law et al.*, 2003]. In addition, empirical, site-specific regressions of approximate soil water potential as a function of soil water content were estimated from TDR measurements and calculated effective soil water potential from predawn leaf water potential measurements. The remaining model parameters were as specified by *Williams et al.* [2001b].

[18] Stand hydraulic parameters were calibrated using measured estimates of daily tree transpiration derived from sap flux density data. We iteratively adjusted the values of the two parameters that determine aboveground and belowground hydraulic resistance in the simulated soil-plant-atmosphere continuum to determine the combination that produced the best agreement between simulated and measured tree transpiration. Parameter values were constrained based on field measurements of leaf specific conductance [*Irvine et al.*, 2004], and final values were selected based on the criteria of minimum root mean square error (RMSE) and highest coefficient of determination ($R^2$) calculated from regressions with measured data. In addition, we calculated relative error rates (in comparison with mean measured fluxes) and partitioned the mean squared error (MSE) into systematic and unsystematic fractions as recommended by *Wallach and Goffinet* [1987, 1989] as cited by *Kramer et al.* [2002].

[19] In summary, sap flux data from each site were used to parameterize the SPA model hydraulics, and a single set of parameters was determined for each site. Eddy flux data were used to evaluate model predictions of total LE and GPP. Three years of sap flux data and eddy flux data (2000–2002) were available for the YS. For the OS, 3 years of sap flux data (2000–2002) were available, but only 2 years of eddy flux data (2000–2001). For the MS, the model was parameterized and evaluated against sap flux and eddy flux data for 2002.

### 2.7. Simulations

[20] To separate relative effects of climatic variation from changes in stand structure, for example, LAI and physiology (plant water relations), we used the model to perform a series of simulations as computational experiments. A base case and three experimental scenarios were simulated (Table 3). Each scenario was applied to the three sites using the 4 years of site-specific climate data (1999–2002), and all 4 years were simulated consecutively for a total of 1461 days. These 4 years represented a 150–200% range of variation of winter precipitation (November–April), 300–600% variation of summer precipitation (May–October), and over 50% variation of annual precipitation (Figure 2). Other climatic vari-

**Table 3.** Summary Descriptions of the Four Simulation Scenarios That Investigate Potential Effects of Climatic Variation Versus Stand Development and Structure on Forest Carbon and Water Fluxes[a]

| Scenario | Description | Daily Leaf Area Phenology | Model Parameters | Soil Moisture Limitation |
|---|---|---|---|---|
| 1 | base case | site-specific leaf area | site-specific parameters | yes |
| 2 | no drought stress | site-specific leaf area | site-specific parameters | no |
| 3 | identical LAI and aboveground structure | MS leaf area | MS parameters | yes |
| 4 | identical aboveground structure and no drought stress | MS leaf area | MS parameters | no |

[a]See section 2.7.

ables showed a range of variation over the 4 years of about 10–20%. Given the close geographic proximity of the YS and MS (~2 km) and the similarity of the climate between the two sites, the YS climate data for 1999–2001 (in addition to the MS 2002 data) were used for MS simulations.

#### 2.7.1. Effects of Climate and Climatic Variation on Carbon and Water Fluxes

[21] The base case (or first) scenario simulated the effects of interannual variation of climate over the 4 years at each of the three sites using site-specific LAI, stand structure, and hydraulic parameters. The second scenario (no drought stress) simulated the removal of soil moisture limitations by resetting soil moisture levels to field capacity (~0.3 $m^3$ $m^{-3}$) while using the same leaf area, stand structure, and hydraulic parameters as the base case scenario. For the YS, these two scenarios were simulated assuming both constant LAI (using the 2002 LAI data) and annually increasing LAI to investigate the added effects of annually increasing leaf area on simulated carbon and water fluxes during the 4 years. Differences between the base case and no drought stress scenarios were used to distinguish the effects of soil moisture limitations (i.e., precipitation) from other climatic effects on carbon and water fluxes.

#### 2.7.2. Effects of Aboveground Stand Structure and Canopy Physiology on Fluxes

[22] Scenario 3 (identical aboveground stand structure and physiology) simulated the effects of replacing the entire aboveground structure of the YS and OS with the aboveground structure (LAI, tree heights, vertical distribution of LAI) and physiology (canopy hydraulic conductance) of the MS. Differences between the base case (scenario 1) and scenario 3 were used to help determine the effects of aboveground stand structure and canopy physiology on carbon and water fluxes. Variations of this scenario were used to distinguish the effects of LAI from other components of stand structure and physiology.

#### 2.7.3. Effects of Root Density and Rooting Depth on Fluxes

[23] Scenario 4 (identical aboveground stand structure and no drought stress) was identical to scenario 3 except that soil moisture limitations were removed (like scenario 2). Under this scenario, virtually unlimited access to soil water effectively minimizes differences in the rooting characteristics among the sites. Thus, differences between scenario 3 and scenario 4 were used to assess effects of differences in soil properties and differences in root density and distribution among the sites.

[24] The scenarios are summarized in Table 3. For scenarios 2–4, the MS was selected as the reference site because it represents the upper limit of LAI and productivity among stands in the region [*Law et al.*, 2003]. Consequently, comparisons with the MS under these scenarios show the maximum potential effect of these simulated changes in stand structure on carbon uptake and water vapor exchange.

### 2.8. Annual Estimates of NEE

[25] Annual estimates of NEE were calculated as the difference between total annual GPP (from the simulations) and annual estimates of $R_e$. Estimates of $R_e$ for each site were calculated as the sum of $R_s$, determined from automated chamber measurements [*Irvine and Law*, 2002], and empirically modeled estimates of $R_f$ and $R_w$ [*Law et al.*, 1999b], plus site-specific estimates of mean annual fine and coarse woody debris decomposition [*Law et al.*, 2003]. Four years of sapwood volume data were used to calculate $R_w$ at the YS. In the absence of similar data for the MS and OS, $R_w$ was assumed constant over the 4 years of the study. Previous studies at the YS and OS indicate that $R_w$ is small fraction of $R_e$ ($\leq$6%) [*Law et al.*, 1999b, 2001c], and this assumption had little impact on the annual estimates of $R_e$.

## 3. Results and Discussion

### 3.1. Model Parameterization

[26] We were able to identify a single pair of hydraulic parameters for each site that was held constant during the multiyear simulations. In contrast, site-specific LAI and total foliar nitrogen varied seasonally. On the basis of the 2002 measurements, total (overstory plus understory) LAI ranged from 0.86 to 1.46 $m^2$ half-surface area of foliage per $m^2$ ground at the YS, 2.19 to 2.74 $m^2$ $m^{-2}$ at the OS, and 2.77 to 3.44 $m^2$ $m^{-2}$ at the MS (Table 2). The parameterizations indicated that rooting was deepest at the OS (1.8 m) and shallowest at the YS (1.0 m). However, fine root biomass in the top meter of soil was highest at the MS and lowest at the OS. Rooting depth and root biomass were assumed constant at the MS and OS during the simulations, but at the YS, because of its stage of development, fine root biomass increased over the 4 years from 450 to 650 g $m^{-2}$, and rooting depth increased from 0.9 to 1.0 m. In terms of water transport, the most conductive stems were at the YS, and the least conductive stems were at the MS. The most resistive roots were at the YS, and the least resistive were at the MS. Leaf specific conductance, which combines the stem and root hydraulic parameters, at the top of the forest canopy was 1.70, 0.28, and 0.20 mmol $s^{-1}$ $m^{-2}$ $MPa^{-1}$ at the YS, MS, and OS, respectively.

### 3.2. Model Comparison With Sap Flux Measurements

[27] Simulations of the YS, MS, and OS indicate that the SPA model can accurately predict seasonal patterns of tree transpiration estimated from measured sap flux using simple parameterizations (Table 4). The SPA model explained 76% to 87% of the daily variation of tree transpiration for years 2000 through 2002 across the three sites. RMSE varied little (0.11–0.20 mm $d^{-1}$) among the seven site-year simulations, suggesting that it may be difficult to resolve model-data discrepancies of less than about 0.1 mm $d^{-1}$. The average relative error (calculated as RMSE/mean daily measured sap flux) between simulated and measured transpiration was 24% (±0.14 mm $d^{-1}$). Furthermore, after partitioning the mean square error into systematic and unsystematic fractions, on average more than half (57%) of the model-measurement discrepancies can be attributed to unsystematic (or random) errors, suggesting that the model is accurately capturing the daily dynamics of tree transpiration (Figure 3).

### 3.3. Model Comparison With Latent Energy Fluxes

[28] Comparisons between simulations of total daily latent energy (LE) fluxes at each of the three sites and

**Table 4.** Comparisons of Daily Estimates of Simulated Tree Transpiration, Total Latent Energy Exchange (Total LE), and Gross Primary Production (GPP) With Measured Values Derived From Sap Flow and Eddy Covariance Measurements[a]

| | | Tree Transpiration | | | | Total LE | | | | GPP | | | |
|---|---|---|---|---|---|---|---|---|---|---|---|---|---|
| Site | Year | $R^2$ | RMSE, mm $d^{-1}$ | Rel. Error, % | Bias, % | $R^2$ | RMSE, mm $d^{-1}$ | Rel. Error, % | Bias, % | $R^2$ | RMSE, g C $m^{-2}$ $d^{-1}$ | Rel. Error, % | Bias, % |
| YS | 2000 | 0.82 | 0.14 | 28 | 17 | 0.79 | 0.36 | 30 | 42 | 0.90 | 0.73 | 24 | 85 |
| | 2001 | 0.87 | 0.13 | 27 | 13 | 0.81 | 0.32 | 32 | 17 | 0.86 | 0.56 | 23 | 48 |
| | 2002 | 0.86 | 0.20 | 30 | 48 | 0.80 | 0.38 | 33 | 24 | 0.90 | 0.49 | 17 | 19 |
| | Avg | 0.85 | 0.16 | 28 | 26 | 0.80 | 0.35 | 32 | 28 | 0.89 | 0.59 | 21 | 51 |
| MS | 2002 | 0.84 | 0.15 | 19 | 32 | 0.50 | 0.62 | 50 | 67 | 0.46 | 0.74 | 12 | 20 |
| OS | 2000 | 0.85 | 0.11 | 19 | 54 | 0.62 | 0.51 | 36 | 81 | 0.40 | 0.56 | 13 | 38 |
| | 2001 | 0.87 | 0.11 | 23 | 65 | 0.64 | 0.36 | 31 | 49 | 0.67 | 1.13 | 22 | 91 |
| | 2002 | 0.76 | 0.14 | 22 | 67 | - | - | - | - | - | - | - | - |
| | Avg | 0.83 | 0.12 | 21 | 62 | 0.63 | 0.44 | 34 | 65 | 0.53 | 0.84 | 18 | 64 |
| Overall Avg | | 0.84 | 0.14 | 24 | 43 | 0.70 | 0.42 | 35 | 47 | 0.70 | 0.70 | 19 | 52 |

[a]RMSE is root mean square error, and the relative error (Rel. Error) is the RMSE as a percentage of the daily mean value determined from field measurements. Bias is the fraction of the mean square error that can be attributed to systematic (as opposed to random) deviations from the measured values. Dashes indicate no data available.

eddy covariance measurements indicate that the model was able to explain 50% (MS) to 81% (YS) of the daily variation of total measured LE among the six site-year combinations with eddy flux data (Table 4). The average relative error between the model and the flux measurements was about 35%, and the overall average RMSE was ±0.42 mm $d^{-1}$. Relative error rates as well as the proportion of the error attributed to systematic differences were smallest at the YS and higher at the MS and OS. Eddy covariance-based estimates of integrated total LE at the YS and MS during non-rain days were higher than simulated estimates (Table 5), although the simulated estimates were within the uncertainty limits for the YS. Because tree transpiration was the largest component of total LE (>50% at each site), the higher relative error rates compared with tree transpiration were most likely associated with other components of total LE such as shrub transpiration, wet canopy evaporation, or soil evaporation.

[29] Because the same model hydraulic parameters were applied to both the understory and overstory canopy layers, we would have expected larger discrepancies between the model and field measurements at the YS (understory LAI 40% of total). However, relative error rates (or discrepancies) for total LE at the YS were smaller than the corresponding relative error rates at either the OS or MS, contrary to our expectations (Table 4). Thus it is unlikely that shrub transpiration, alone, could explain the discrepancies in simulated versus measured total LE, especially at the OS and MS.

[30] Evaporation from soil surfaces could also be contributing to the discrepancies between the flux measure-

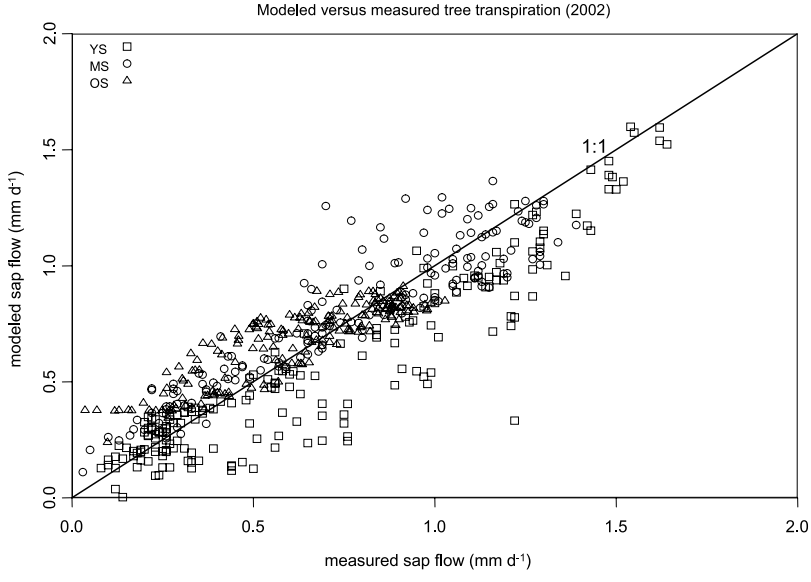


**Figure 3.** Simulated versus measured tree transpiration during 2002, the only year with measured sap flux data for each site. The 1:1 line indicates that the simulated values are relatively unbiased.

**Table 5.** Integrated Water Vapor Fluxes and Annual Carbon Fluxes Derived Eddy Covariance Measurements and Simulations[a]

| | LE,[b] mm | | GPP (g C $m^{-2}$ $yr^{-1}$) | | NEE,[c] g C $m^{-2}$ $yr^{-1}$ | |
|---|---|---|---|---|---|---|
| Site (Year) | Measured | Modeled | Measured | Modeled | Measured | Modeled |
| YS (2001) | 224 ± 36 | 199 | 704 ± 168 | 674 | 45 ± 6 | 48 |
| YS (2002) | 269 ± 43 | 234 | 809 ± 193 | 828 | 113 ± 15 | 192 |
| MS (2002) | 296 ± 51 | 241 | 1360 ± 333 | 1539 | 371 ± 53 | 516 |

[a]For the OS, insufficient eddy flux data were available for 2001 to estimate annual fluxes, and no eddy flux data were available for 2002.
[b]Rain days were excluded from the integrated estimates of LE because of the effects of rain droplets on the eddy covariance instrumentation. Thus the LE estimates are not true annual estimates.
[c]Modeled estimates of NEE are determined from simulated estimates of GPP plus empirical estimates of ecosystem respiration derived from measurements of soil $CO_2$ efflux, foliage respiration, sapwood respiration, and woody litter decomposition (see section 2.8).

ments and the model. *Williams et al.* [2001b] reported good agreement between the SPA model and measurements of soil evaporation at the OS during August 1997. In the current study, however, we utilized field measurements of tree transpiration and expanded the number of sites and the number of years of data used for the model-measurement comparison. The largest discrepancies between the eddy covariance-based estimates of total LE and the model occurred usually during June and July, when the model underestimated total LE by $\sim$1 mm $d^{-1}$ or >40% at the MS. Simulated soil evaporation at the MS during the summer months was relatively constant and averaged $\sim$0.2–0.3 mm $d^{-1}$. Although simulated soil evaporation compared favorably with LE fluxes measured by a subcanopy eddy covariance system installed at the MS during August–September 2002, no measurements were available from earlier in the summer when measurement-model discrepancies were larger. Thus, to further improve the model's capability to simulate soil evaporation at these sites, additional measurements of soil evaporation will be needed that span the growing season.

[31] Another possible source for discrepancies between simulated and measured total LE is differences in the sampling footprint used to calculate tree transpiration from sap flow measurements and the sampling footprint for the eddy covariance measurements, even though a rigorous approach was used to scale the sap flow measurements to site [*Irvine et al.*, 2002]. Scaled estimates of transpiration are sensitive to the measured basal area and sapwood area relationships in the field plots, and although the field plots were chosen to be representative of each site, structural characteristics of the plots may not match those of the area being integrated by the eddy covariance technique. Other recent studies have also reported difficulties in reconciling sap flow measurements with latent energy flux measurements using the eddy covariance technique [*Wilson et al.*, 2001; *Meiresonne et al.*, 2003], and we submit that the footprint issue requires further investigation.

### 3.4. Model Comparison With GPP Estimates Derived From Eddy Flux Data

[32] The average relative error between modeled and measured estimates of daily GPP among the three sites was 19%, and RMSE varied by about a factor of 2 from 0.49 g C $m^{-2}$ $d^{-1}$ to 1.13 g C $m^{-2}$ $d^{-1}$ (Table 4). Simulations of the YS, though, explained considerably more day-to-day variation in GPP than at either the MS or OS, and roughly half of the mean square error could be attributed to systematic differences between the modeled and measured values. Although the overall relative error between the eddy covariance-based estimates and simulated estimates of GPP was generally good (19%, Table 4), the lower $R^2$ values and higher bias indicate that the model misses some of the day-to-day variation associated with the carbon dynamics of the sites. In general, though, as time series data are aggregated over longer periods, discrepancies between predicted and measured values are substantially reduced because differences due to unsystematic (or random) variation tend to cancel one another [*Goulden et al.*, 1996; *Moncrieff et al.*, 1996].

[33] Annual estimates of simulated GPP were well within the uncertainty limits of the flux measurements (Table 5). Simulated estimates were higher than the measured estimates in 2002 but lower than the measured estimate for the YS in 2001. Thus, although the model may be underestimating total LE at the study sites, the model appears suitable for simulating seasonal and annual responses of transpiration and GPP to changes in climate and climatic variation.

### 3.5. Simulation Scenarios

#### 3.5.1. Effects of Climate and Climatic Variation

[34] Precipitation at the sites varied $\sim$55% over the 4 years: 1999 was the wettest year followed by 2001, 2000, and 2002 was the driest year. When LAI at the YS was held constant over the 4 years to separate effects of climatic variation from changes in leaf area, GPP was highest during 1999 and lowest in 2002, following interannual trends in total annual precipitation. At the MS and OS, however, annual GPP was highest in 1999 and lowest in 2001, which mirrored the interannual pattern of soil water recharge from winter precipitation.

[35] Despite similar climate across the three sites, the base case simulations (scenario 1) showed that interannual variation of GPP differed by site in response to climatic variation over the 4-year period (Table 6, Figure 4, base case). Annual GPP in the base case simulations varied <10% per year at the OS to >50% per year at the MS across the 4 years, implying that interannual variation of GPP among the 4 years was highest at the MS and lowest at the OS. Under the base case scenario with constant LAI, interannual variation of GPP at the YS across the 4 years was 19%. The interannual variation of GPP at the MS was similar to the interannual variation of precipitation, and the interannual variation of GPP at the YS was comparable to that of the MS when simulations increased the LAI at the

**Table 6.** Annual Summaries of the Simulated Carbon and Water Vapor Fluxes From the Simulations[a]

| Scenario | | Total LE, mm $yr^{-1}$ | | | Tree Transpiration, mm $yr^{-1}$ | | | GPP, g C $m^{-2}$ $y^{-1}$ | | |
|---|---|---|---|---|---|---|---|---|---|---|
| | | YS | MS | OS | YS | MS | OS | YS | MS | OS |
| Base case | mean | 309 \| 279 | 304 | 299 | 136 \| 115 | 171 | 161 | 801 \| 679 | 1401 | 1098 |
| | std dev | 31 \| 17 | 37 | 13 | 13 \| 16 | 34 | 9 | 55 \| 93 | 219 | 30 |
| | percent variation | 33 \| 17 | 40 | 13 | 28 \| 38 | 77 | 17 | 19 \| 45 | 53 | 7 |
| No drought stress | mean | 434 \| 385 | 442 | 327 | 241 \| 204 | 309 | 187 | 1013 \| 846 | 1886 | 1168 |
| | std dev | 18 \| 32 | 20 | 14 | 4 \| 32 | 11 | 6 | 8 \| 132 | 49 | 15 |
| | percent variation | 11 \| 17 | 12 | 11 | 5 \| 52 | 10 | 9 | 2 \| 55 | 7 | 3 |
| | percent change | 40 \| −11 | 45 | 9 | 78 \| −15 | 80 | 16 | 26 \| −17 | 35 | 6 |
| Identical LAI and aboveground structure | mean | 305 | 304 | 369 | 191 | 171 | 227 | 1413 | 1401 | 1648 |
| | std dev | 25 | 37 | 20 | 23 | 34 | 22 | 100 | 219 | 83 |
| | percent variation | 23 | 40 | 16 | 37 | 77 | 31 | 21 | 53 | 14 |
| | percent change | −1 | - | 23 | 40 | - | 42 | 76 | - | 50 |
| Identical aboveground structure and no drought stress | mean | 392 | 442 | 438 | 283 | 309 | 289 | 1686 | 1886 | 1816 |
| | std dev | 20 | 20 | 10 | 9 | 11 | 10 | 24 | 49 | 30 |
| | percent variation | 14 | 12 | 5 | 9 | 10 | 10 | 4 | 7 | 4 |
| | percent change | 27 | 45 | 46 | 108 | 80 | 27 | 110 | 35 | 65 |

Percent variation describes the relative range of variation over the four simulated years, 1999–2002.

[a]Percent change describes the relative difference between a given scenario and the base case scenario. Dashes indicate not applicable. The vertical bars for the YS separate the results for the constant LAI simulations on the left from the annually adjusted LAI simulations on the right.

YS to match the measured LAI. In contrast, the interannual variation of GPP at the OS was much less than the interannual variation of precipitation. Interchanging climate driver data among the sites had little effect on mean annual GPP at either the OS or MS and reduced mean GPP at the YS by no more than 5%.

[36] Seasonally, interannual variation of GPP at the MS was most pronounced during July–September, while variation at the YS was most noticeable earlier during May–July (Figure 4, base case). At the OS, the interannual variation appeared uniformly distributed throughout the year.

[37] Base case simulations (scenario 1) of tree transpiration and total LE showed noticeably more interannual variation than GPP because of larger interannual variation in LE and precipitation earlier in the year (Table 6, Figure 5, base case). Among-site differences in transpiration were substantially smaller than the corresponding differences in GPP (Table 6): about 25% for mean annual tree transpiration (assuming constant LAI at the YS) and less than 5% for mean annual total LE.

[38] Increased soil water availability at the MS and YS, under scenario 2 (no drought stress), resulted in large increases in mean annual tree transpiration of >75% and increased total annual LE by ≥40% (Table 6). Moreover, the increased tree transpiration and total LE were most evident during the period of otherwise maximum drought stress (Figure 5). The simulations suggest that increased soil moisture from precipitation during the growing season would probably have a greater effect on carbon and water fluxes in these forests than increased precipitation at other times of the year [*Goldstein et al.*, 2000; *Xu and Baldocchi*, 2004]. Mean simulated tree transpiration and total LE at the OS, on the other hand, increased only by about 16% and 9%, respectively, reflecting a smaller effect of increased soil moisture in the upper soil layers at this site. These results are consistent with those of *Irvine et al.* [2004], who determined that approximately 79% of water used during the summer months of 2002 at the YS was extracted from a depth of 80 cm or less, whereas almost half (47%) of the water extracted at the OS during the same months came from below 80 cm depth.

[39] Simulations that increased soil water availability and eliminated seasonal drought stress (scenario 2) increased mean annual GPP at the YS and MS by 26% and 35%, respectively (Table 6). Furthermore, simulations clearly show that the increased GPP occurs during the late summer and early fall months when drought stress would normally be experienced (Figure 4). In contrast, the simulated response of the OS was small: Mean annual GPP increased by 6%, and the seasonal pattern of GPP was similar to that of the base case scenario. Therefore the benefits of increased soil water availability had a much bigger effect at the YS and MS than at the OS.

[40] Increased soil water availability subsequently reduced interannual variation of GPP to similarly low levels at all three sites (2–7%, Table 6). Hence the simulations confirm that interannual variation of precipitation is an important causal factor controlling GPP and probably accounts for most of the interannual variability of GPP in these forests. Under scenario 2, though, after removing the variation of rainfall, the dominant sources of interannual climatic variation were radiation inputs and temperature, and the interannual variation of radiation probably had a larger effect on the interannual variation of GPP at the MS (7%) because it had highest LAI among the three sites. In contrast, the YS experienced the least interannual variation of GPP (2%, assuming constant LAI), and although the interannual variation of solar radiation was higher at the YS compared to the OS, even during the year with the lowest solar radiation inputs (2001), there was sufficient radiation to effectively saturate the lower LAI canopy of the YS.

[41] Other studies reached similar conclusions regarding effects of interannual variation of climate on carbon uptake in forests. For example, *Barford et al.* [2001], in a 9-year study of eddy covariance data from a deciduous hardwoods stand in Massachusetts, attributed interannual variation of carbon uptake and net carbon exchange to the variation of climatic characteristics such as cloudiness and low temper-

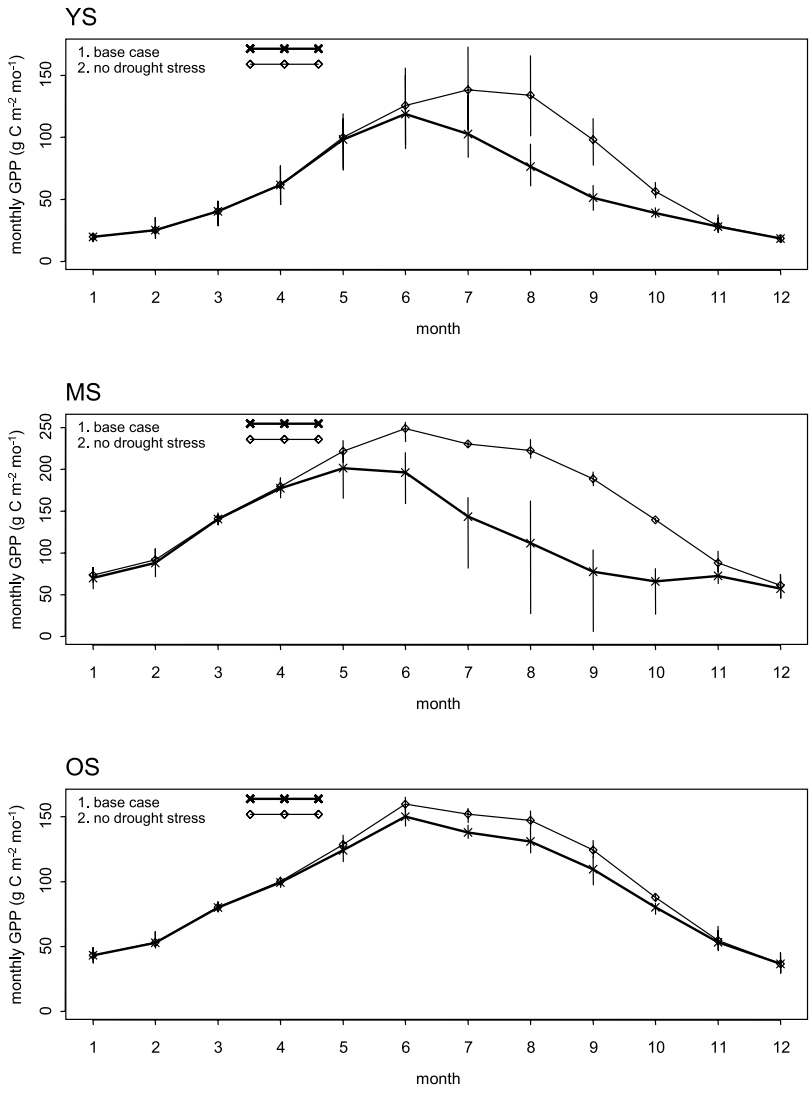


**Figure 4.** Monthly GPP under the base case and no drought stress scenarios showing effects of seasonal drought at the sites. Differences between the two curves are an estimate of the reduction in GPP caused by drought. Vertical bars show the range of variation over the four simulated years, 1999–2002.

atures, which influenced growing-season length. *Griffis et al.* [2003], based on 6 years of eddy covariance data, associated higher GPP with warmer climatic conditions at an aspen site in Saskatchewan, Canada. However, to our knowledge, our study is the first to suggest that gross carbon uptake of nearby stands of the same forest type, with largely similar climate, can have substantially different sensitivities to interannual variation of climate.

### 3.5.2. Effects of Aboveground Stand Structure and Canopy Physiology

[42] Mean annual simulated GPP during 1999–2002 was highest at the MS and lowest at the YS, consistent with the rank differences in LAI among the sites (Table 2). Mean annual GPP was 1401, 1098, and 679 g C $m^{-2}$ $yr^{-1}$ at the MS, OS, and YS, respectively (Table 6, base case). When LAI was held constant at the YS (using the 2002 LAI), mean annual GPP increased by ~18% to 801 g C $m^{-2}$ $yr^{-1}$.

[43] Increasing the LAI at the YS to match interannual changes in measured values during the base case simulations produced higher interannual variation of the fluxes of carbon and water vapor (Table 6). For GPP, interannual variation increased from 19% to 45%, and the pattern of GPP relative to the pattern of annual precipitation was reversed. GPP was highest in 2002 and lowest in 1999, which reflected the importance of stand leaf area in determining gross carbon uptake. Similar responses to increasing LAI during the 4-year simulations were also noted for tree transpiration and total LE. Under scenario 2 (no drought stress), the interannual variation of GPP over the 4-year period increased despite the stabilizing effect of increased soil water availability (Table 6). Thus the simulations suggest that increases in leaf area, alone, may have a tendency to increase the sensitivity of a stand to interannual variation of climate, at least in low LAI systems like our

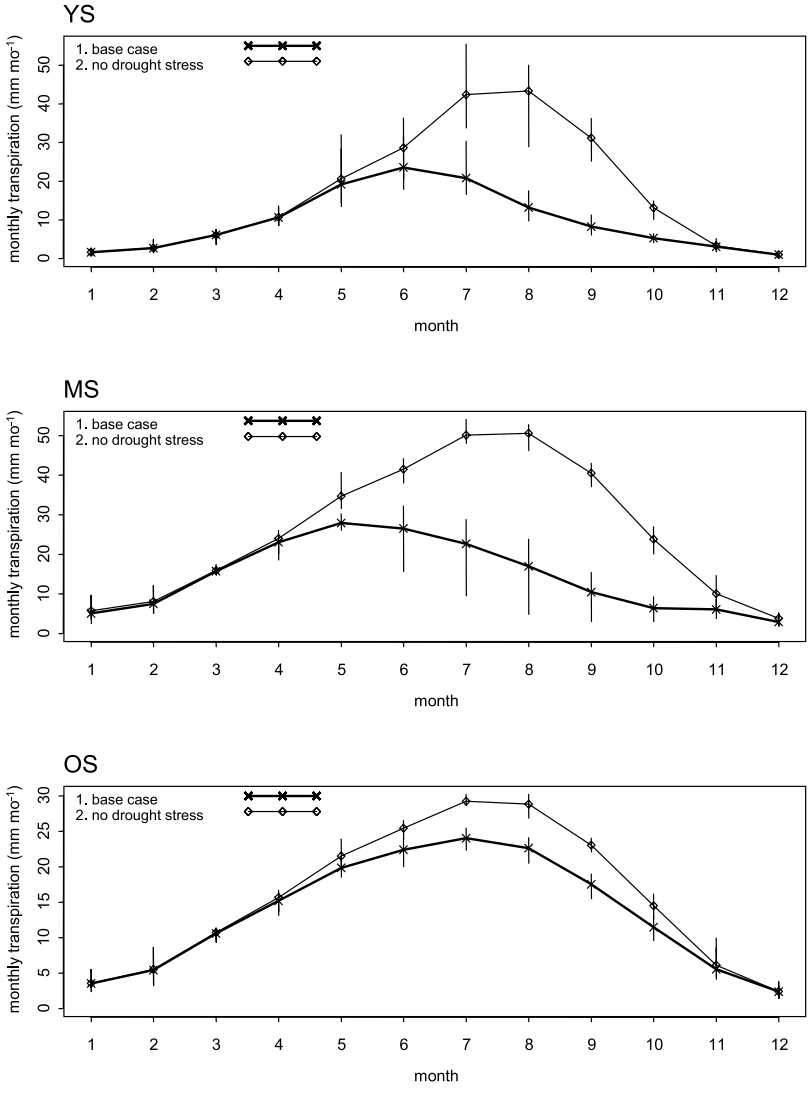


**Figure 5.** Monthly tree transpiration under the base case and no drought stress scenarios, showing effects of seasonal drought at the sites. Differences between the two curves are an estimate of the reduction in GPP caused by drought. Vertical bars show the range of variation over the four simulated years, 1999–2002.

sites. In stands with higher LAI, though, changes in leaf area could produce feedbacks in other components of the stand's overall energy balance.

[44] Scenario 3 (identical aboveground structure and physiology) replaced the aboveground structure of the YS and OS with the LAI, foliage distribution, and canopy hydraulic conductance of the MS. Most of among-site differences in GPP can be explained by differences in stand structure and canopy physiology (Figure 6, third plot). Compared to the base case, mean annual GPP increased 76% and 50%, respectively, at the YS and OS, and differences in mean annual GPP among the three sites were reduced to 18% (Table 6). Additional simulations at the OS, which separated the effects of LAI, hydraulic conductance, and vertical canopy structure, revealed that 16% of the 50% increase in mean GPP could be attributed to the increased LAI, and most of the remainder was caused more by the simulated changes in height and vertical distribution of foliage rather than the simulated changes in hydraulic properties of the sites. In contrast, at the YS, 61% of the 76% increase in mean GPP was related to the increased LAI, with most of the remainder being attributed the simulated changes in height and vertical distribution of foliage, which increased absorption of radiation by the plant canopies.

[45] Simulated responses of tree transpiration and total LE to changes in aboveground stand structure under scenario 3 differed somewhat from those of GPP (Table 6, Figure 7). Mean annual tree transpiration at the YS and OS increased by ~40% relative to the base case scenario, but in contrast with simulated GPP, differences among the sites in mean annual transpiration increased as well, suggest-

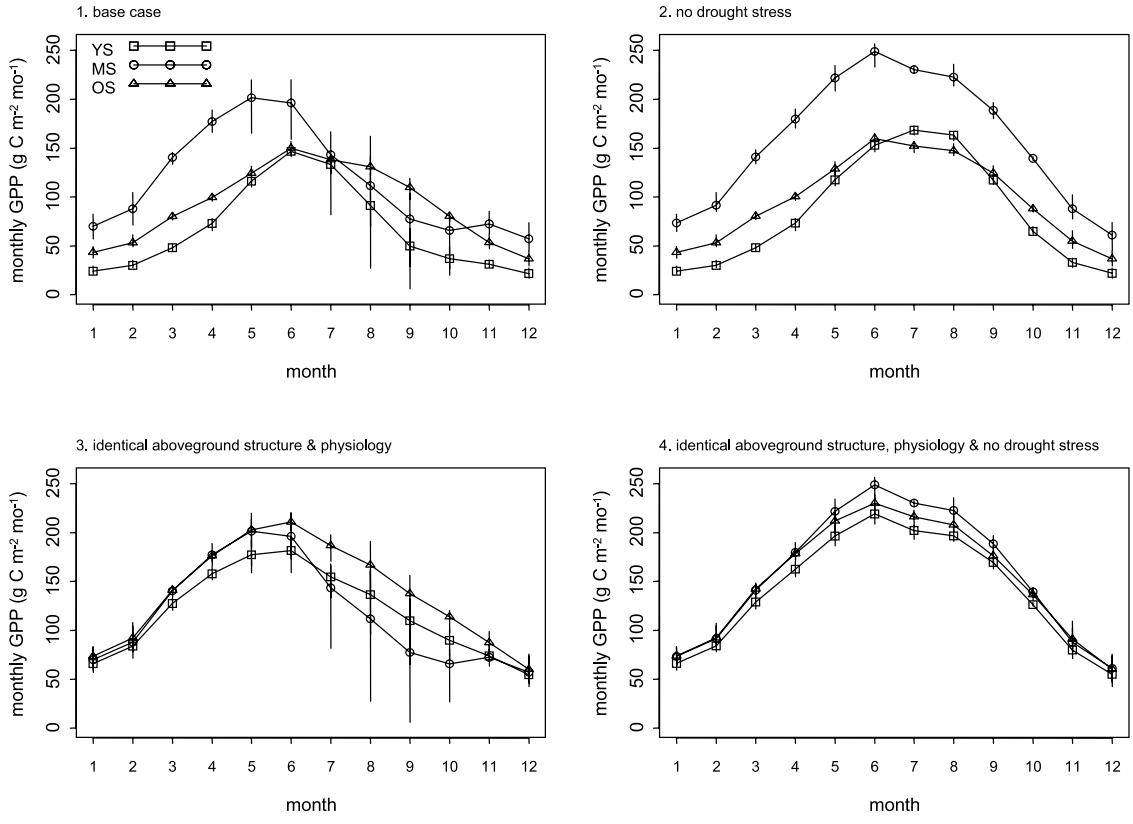


**Figure 6.** Comparisons of monthly GPP among the four simulated scenarios for each of the three sites. Vertical bars show the range of variation over the four simulated years, 1999–2002. The simulations for the YS assume that LAI was constant over the 4 years.

ing that belowground differences were contributing among-site differences.

[46] Most of the seasonal variation of the fluxes of carbon and water vapor was evident during the months of July–October (Figures 6 and 7), similar to the base case scenario. Furthermore, despite identical aboveground structure at each of the sites, there were still distinct differences in the interannual variation of GPP among the sites, which were 53%, 21%, and 14% at the MS, YS, and OS, respectively (Table 6), further suggesting that belowground site differences were responsible for the pattern of interannual variation. Similarly, the same pattern of interannual variation among the three sites was evident for tree transpiration and total LE.

[47] Other simulated changes in aboveground structure besides LAI influenced the hydraulic properties of both stands but had a bigger relative impact on GPP at the OS than at the YS. The net effect of altering the tree heights and hydraulic conductance increased overall canopy hydraulic conductance at the OS but decreased canopy conductance at the YS. Hydraulic limitations have been proposed as an explanation for reduced productivity in older trees [e.g., *Yoder et al.*, 1994; *Ryan and Yoder*, 1997], but see *Ryan et al.* [2004]. The effects of these simulated changes are a logical extension of previous research on hydraulic limitations [e.g., *Waring and Running*, 1978; *Zimmermann*, 1983; *Yoder et al.*, 1994; *Ryan and Yoder*, 1997] and have been discussed previously by *Williams et al.* [2001a].

[48] Our simulations also suggest that rapidly developing stands, such as the YS, may be prone to higher interannual variation of GPP than stands with stable LAI (Table 6, base case). Moreover, the interannual variability of GPP increased in the simulations that removed soil moisture limitations at the YS (no drought stress scenario). In the absence of water limitations, GPP is constrained on an annual basis mostly by the amount of PAR intercepted by the foliage, and over the 4-year simulation, the fraction of absorbed PAR at the YS increased by about 40%, which explains most of the increased variability of GPP despite the otherwise stabilizing effect of increased soil water availability. After accounting for the increase in LAI, the remaining variation (15%) was similar to the variation of the base case scenario with stable LAI (19%) and can be attributed to interannual climatic variation. In general, though, our results suggest that following disturbance, young, rapidly developing stands may be more sensitive to variations in climatic conditions than stands with more stable LAI, which, in turn, could cause these stands to shift, on an annual basis, from net sources or net sinks of carbon, assuming that the interannual variation of GPP is larger than the interannual variation of ecosystem respiration [*Law et al.*, 2001c, 2003]. This possibility is discussed in more detail below.

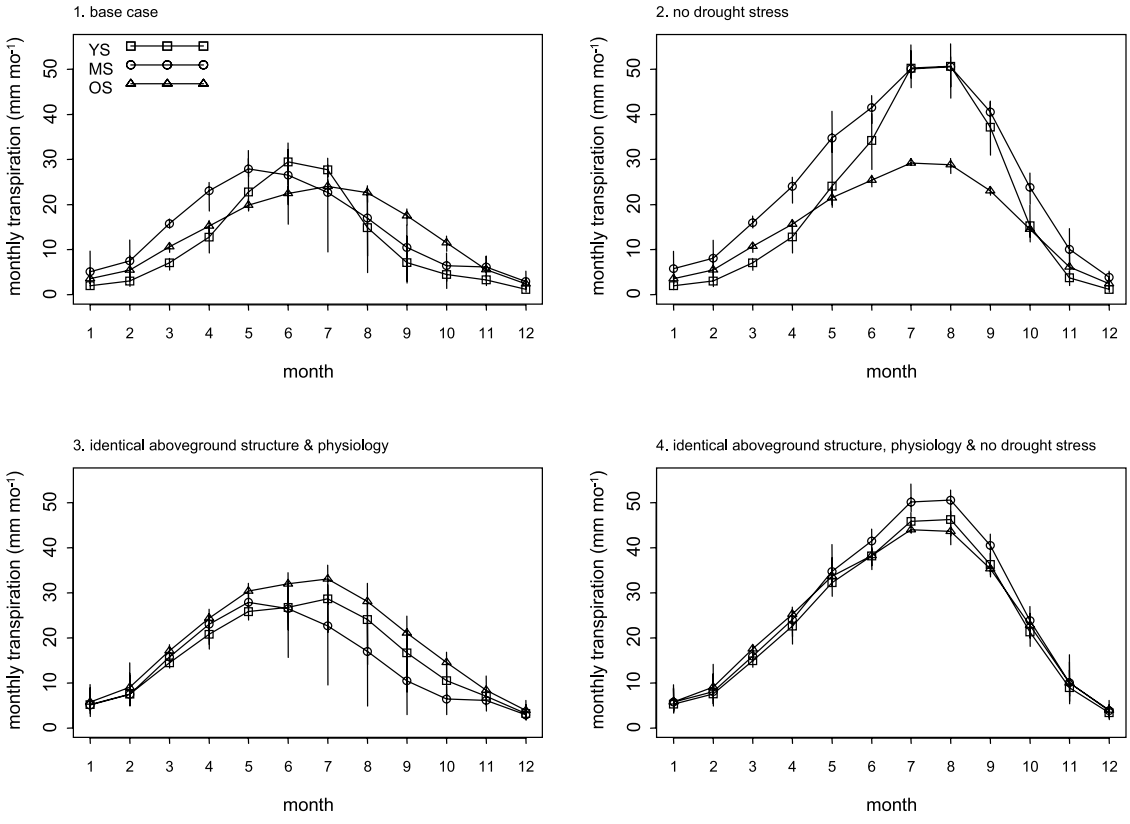


**Figure 7.** Comparisons of monthly tree transpiration among the four simulated scenarios for each of the three sites. Vertical bars show the range of variation over the four simulated years, 1999–2002. The simulations for the YS assume that LAI was constant over the 4 years.

[49] Our purpose for simulating changes in stand structure, though, was to investigate possible explanations for the differential response and sensitivity among the sites to increased precipitation and interannual climatic variation, and although the simulated changes in aboveground stand structure and physiology had a large impact on GPP at the sites, they had little effect on the interannual variation of GPP. The range of interannual variation among the sites (with identical aboveground structure) was similar to the range of variation under the base case scenario, and the rank differences among the three sites were the same (Figure 6, Table 6). Hence we concluded that differences in aboveground stand structure and physiology, alone, could not explain the site-specific differences in sensitivity to interannual climatic variation.

### 3.5.3. Effects of Root Density and Rooting Depth

[50] Under scenario 3 (identical aboveground structure and physiology), the only differences between the sites were those differences related to belowground structure (fine root density and distribution) and to physical soil properties, which were minor (Table 1), and the simulations under scenario 4 (identical aboveground structure and no drought stress) effectively minimized differences in carbon uptake and water vapor exchange among the three sites (Figure 6). Virtually unlimited soil water availability increased mean annual GPP at the YS and OS by 19% and 10%, respectively, compared with the previous scenario, and the variation of mean annual GPP among the three sites was reduced to 12% (Table 6). Furthermore, the interannual variation of GPP was similar among the sites and ranged from 4 to 7%. Hence the simulated increase in soil water availability compensated for differences in belowground structure among the sites and effectively eliminated differences in root density and distribution. Additional simulations using identical climate data for each site (rather than site-specific data) produced virtually identical interannual variation, 7.5–7.7% among the three sites. Thus most of the differences in interannual variation of GPP among the sites, evident in the previous simulations, could be attributed to site-specific differences in fine root density and root distribution. Therefore the smaller interannual variation of GPP at the OS evident in the base case simulations (Figure 6) can be explained by root systems at the site that can access water deeper in the soil profile.

[51] The effects of scenario 4 on tree transpiration and total LE were similar to those of GPP. Mean annual fluxes increased and differences among the sites decreased (Figure 7). Differences in interannual variation of transpiration and total LE among the sites were also reduced (Table 6), and although most of the among-site differences of total LE were related to differences in tree transpiration, some of the differences were also related to soil evaporation.

[52] An alternative explanation for lower interannual variation of GPP at the OS and the site's modest response

to simulated increased soil water availability could be that soil moisture levels at the OS were higher than at either the YS or MS. Precipitation, though, at the three sites was similar (Figure 2), and measurements of soil water content during the growing season in the topmost meter of soil indicated that soil moisture was also similar among the three sites (J. Irvine, unpublished data, 2002). Furthermore, measured and simulated soil water content values were also comparable. However, predawn foliage water potential measurements during the 1999–2002 growing seasons showed that the OS had higher levels of available soil water than either the YS or MS, which suggested that OS experienced less drought stress than the other two sites [*Irvine et al.*, 2004]. Consequently, among-site differences in soil characteristics and soil water content in the top meter of soil were minor and do not explain the sites' differential response to interannual climatic variation or a simulated increase in precipitation.

[53] Simulation scenarios 3 and 4 provide compelling evidence that the most likely explanation for both the modest reduction in GPP at the OS in response to drought as well as the site's lower interannual variation of GPP is that tree roots at the site are able to access soil water from deeper in the profile, whereas tree roots at the YS and MS cannot. In addition to the simulation results, there are some empirical data that support the conclusion of a greater rooting depth at the OS. *Irvine et al.* [2002] concluded that a deeper rooting depth at the OS (compared to the YS) was the most likely explanation for less negative soil water potentials at the OS in an empirical study of sap flux measurements and soil $CO_2$ fluxes at the YS and OS. Furthermore, analyses of stable oxygen isotope data, although not conclusive, indicated that the $\delta^{18}O$ signature of xylem water in trees at the OS was more similar to that of nearby spring water than the corresponding isotope signature of soil water in the surface layers, which also supports the argument that trees at the OS have access to and are using water from deeper in the soil profile [*Bowling et al.*, 2003].

[54] A comparatively shallower rooting depth parameter value for the YS is reasonable given the site's stage of development following disturbance [*Law et al.*, 2001c]. A similarly shallow rooting depth parameter value, though, for the MS raises questions regarding whether the root system has had adequate time to develop or whether there are site factors that could be limiting root system development. Ordinarily, individual ponderosa pine trees would be expected to establish their root systems within a few years, and pure stands would have fully developed root systems within a few decades [*Oliver and Ryker*, 1990; *Stone and Kalisz*, 1991]. An analysis of empirical height-age relationships similar to that used to develop site index curves for forestry applications [e.g., *Meyer*, 1938] suggests that both the MS and YS may be poorer quality sites compared to the OS, which might reflect possible differences in rooting depths at the sites. However, these site differences are probably not nutrient related. Recently, *Kelliher et al.* [2004] reported that concentrations of total carbon (C), total nitrogen (N), and mineral N in the top 10 cm of soil, where most fine roots are located, were similar at YS and OS. At deeper depths, though, the YS had higher concentrations of total C and total N but not mineral N. Nitrogen mineralization rates at the two sites were also similar, and they concluded that mineralization rates of both soil and litter C at the sites was limited more by the availability of water than by N [*Kelliher et al.*, 2004]. It is possible, though, that some physical obstruction, perhaps related to site geology or topography, may be restricting root system development at the MS.

[55] In general, our simulations support the view that older forest stands, with well-established root systems, are better able to buffer effects of intra-annual and interannual variation of climate than younger stands with less-developed root systems that grow in semi-arid regions like central Oregon. One concern of a potential change in climate is that there will be increased variation in individual extreme precipitation events as well as increased variation in total annual precipitation [*Easterling et al.*, 2000]. Our simulations suggest that younger forests, under circumstances of increased climatic variability, would be subject to higher interannual variation of gross carbon uptake and be more susceptible to climatic extremes. In a recent review, *Weltzin et al.* [2003] voiced similar concerns about the potential effects of changes in precipitation regimes on ecological systems. In addition, much of the western United States (including semi-arid regions with ponderosa pine) is subject to both natural (e.g., wildfire) and human-caused (e.g., logging) disturbances, which have a direct impact upon the stage of development and structure of forested ecosystems. Thus, in addition to the ecological implications of our results for ecosystem functioning, our simulation results may have further implications for forest management policies.

### 3.6. Implications for Net Ecosystem Exchange

[56] The model-based annual estimate of NEE for the YS in 2001 compared favorably with the estimates derived from eddy flux data (Table 5). However, for 2002, modeled NEE was considerably larger than the flux-based estimates. At the MS, the larger modeled NEE (compared with measured) is related to the much higher simulated GPP at the site. At the YS, it is unclear why modeled NEE was higher than measured NEE in 2002, but it may be related to a higher estimate of foliage respiration ($R_f$) in 2002 than 2001, although $R_e$ is similar between the two years (Table 7).

[57] At the OS, NEE was lowest in 2000 and highest in 1999, but among the 4 years, the site was a consistent and stable net carbon sink (Table 7). In contrast, NEE at the YS varied widely. In 1999, the site was a small net carbon source but was a net sink for carbon thereafter. Similarly, the 2 years of available data for the MS suggest that NEE at the site was highly variable and that the site was a net sink for carbon. Across the 4 years, interannual variation of $CO_2$ fluxes from the soil surface ($R_s$) was similar among the three sites and accounted for >70% of annual $R_e$ at the YS and OS and ~64% at the MS. Consequently, interannual variation of $R_e$ at the sites was controlled mostly by interannual variation of $R_s$. At the YS, the variation of $R_e$ was also controlled in part by interannual variation of $R_f$ as leaf area increased. Because GPP at the OS was stable over the

**Table 7.** Annual Estimates of Net Ecosystem Exchange (NEE) Determined From Simulations of GPP and Annual Estimates of Respiration Derived From Measurements at Each of the Study Sites[a]

| | YS | | | | | MS | | | | | OS | | | | |
|---|---|---|---|---|---|---|---|---|---|---|---|---|---|---|---|
| | $R_s$ | $R_f$ | $R_e$ | GPP | NEE | $R_s$ | $R_f$ | $R_e$ | GPP | NEE | $R_s$ | $R_f$ | $R_e$ | GPP | NEE |
| 1999 | 453 | 111 | 590 | 573 | −17 | - | - | - | 1565 | - | 497 | 141 | 69 | 1126 | 436 |
| 2000 | 377 | 142 | 545 | 643 | 98 | - | - | - | 1472 | - | 587 | 142 | 781 | 1101 | 320 |
| 2001 | 452 | 147 | 626 | 674 | 48 | 575 | - | 925 | 1026 | 101 | 488 | 148 | 688 | 1049 | 361 |
| 2002 | 430 | 180 | 636 | 828 | 192 | 673 | 268 | 1023 | 1539 | 516 | 519 | 147 | 718 | 1117 | 399 |
| Mean | 428 | 145 | 599 | 679 | 80 | 624 | - | 974 | 1401 | 309 | 523 | 144 | 719 | 1098 | 379 |
| Std dev | 36 | 28 | 41 | 108 | 88 | 69 | - | 69 | 253 | 293 | 45 | 3 | 44 | 35 | 50 |
| Percent variation | 20 | 62 | 17 | 45 | n.a. | 17 | - | 11 | 53 | 410 | 20 | 5 | 14 | 7 | 36 |

[a]Units are g C $m^{-2}$ $yr^{-1}$. $R_s$, $CO_2$ efflux from the soil surface; $R_f$, foliage maintenance respiration; $R_e$, whole ecosystem respiration, $R_e = R_s + R_f +$ sapwood respiration ($R_w$) + annual decomposition of woody material (see section 2.8). NEE = GPP − $R_e$. Dashes indicate no data available.

4 years, interannual variation of NEE at the site was determined mostly by the interannual variation of $R_e$, whereas the interannual variation of GPP probably had a much bigger effect on the interannual variation of NEE at the YS and MS (Table 7).

[58] Determining the sign, magnitude, and interannual variation of NEE in various ecosystems is critical to developing a better understanding of global carbon budgets [*Schimel et al.*, 2001]. Our results suggest that the controls on the interannual variation of NEE in ponderosa pine forests, even with similar climate, are not simple and consistent across age classes but may differ according to development stage. Although the robustness of the NEE calculations using our approach is unclear, the apparent transition of the YS from a net carbon source to a net carbon sink highlights the importance of forest recovery following disturbance in determining terrestrial carbon balances [*Law et al.*, 2001c; *Schimel et al.*, 2001; *Goodale et al.*, 2002].

[59] Our results contribute to the debate regarding the relative importance of $R_e$ versus GPP in controlling the interannual variation of NEE. Some studies of forests suggest that $R_e$ varies more than GPP on an annual basis [*Valentini et al.*, 2000; *Janssens et al.*, 2001; *Valentini et al.*, 2003]. Other studies indicate that GPP varies more than $R_e$ [*Arain et al.*, 2002; *Aubinet et al.*, 2002], while other studies show that the interannual variation of $R_e$ and GPP is roughly the same [*Barford et al.*, 2001; *Suni et al.*, 2003; *Wang et al.*, 2004]. Our results are important because they suggest that in forests with similar climate, the relative importance of $R_e$ and GPP may depend upon the development stage of the forest.

## 4. Conclusions

[60] Meteorological data collected at the study sites indicated that precipitation was the dominant source of climatic variation over the 4-year period, 1999–2002, and that the variation in annual precipitation exceeded 50%, while summer precipitation varied more than six-fold. Model simulations at the three sites suggested that interannual variation of GPP over the 4 years ranged from 7% (OS) to >50% (MS). Simulations that assessed the effects of seasonal drought at the sites suggested that the YS and MS were relatively more constrained by seasonal drought stress than the OS throughout the 4-year period, such that interannual variation of climate had a larger effect on the YS and MS and very little effect on GPP at the OS, which was buffered by deeper rooting. At the rapidly developing YS, changes in stand structure, such as increasing leaf area associated with vigorous growth, appear to have larger effects on carbon and water fluxes than variation in climate, although effects of these changes may interact with other biotic effects including shifts in carbon allocation and whole-tree hydraulic conductance. Interannual variation of NEE, based on simulations of GPP and empirical estimates of $R_e$, was also less variable at the OS than at the other two sites, and whereas interannual variation of NEE at the OS during the 4 years was probably controlled mostly by the variation of $R_e$, interannual variation in NEE at the YS and MS appeared to be more strongly controlled by the interannual variation of GPP.

[61] Our results suggest that the interannual variation of precipitation is probably the dominant control on carbon and water vapor fluxes in temperate coniferous forests growing in semi-arid regions. Additionally, older forest stands with well-established root systems appear to be better able to buffer the effects of both seasonal drought stress and interannual climatic variation than younger stands. In many forested landscapes, mosaics of different forest development stages are present because of the effects of wildfire and timber harvesting (Figure 1). Carbon uptake and water vapor exchange among stands with different structural characteristics and stages of development can show varying responses to the interannual variation of climate, and the aggregate pattern of carbon and water fluxes at the landscape level will likely depend upon the distribution of different development stages. If there is a higher proportion of younger stands in the landscape because of disturbances like intensive harvesting or wildfire, then GPP across the landscape is likely to undergo large interannual variations in response to climate, whereas a higher proportion of old stands would probably dampen the interannual fluctuation of GPP. In western North America where ponderosa pine forests are common, there are relatively few old stands; thus the interannual variation of GPP in this region is likely to be large. Because interannual variation of NEE in younger pine forests is probably more strongly related to the interannual variation of GPP than $R_e$, NEE across the region is also likely to vary considerably in response to the interannual variation of climate.

[62] **Acknowledgments.** This study was funded by NASA (grant NAG5-11231), a study on regional carbon dioxide and water vapor exchange over heterogeneous terrain, and the Department of Energy (DOE grant FG0300ER63014) study on carbon dioxide and water vapor exchange in successional stages of Pacific Northwest forest ecosystems. We gratefully acknowledge Adam Pfleeger for invaluable field and laboratory assistance, and tree climbers from the EPA, Corvallis, for their installation of sap flux probes at the old site. The authors are also grateful for the helpful comments and suggestions from two anonymous reviewers. In addition, the first author wishes to thank R. H. Waring for his many ideas and helpful suggestions. We appreciate the Sisters Ranger District of the U.S. Forest Service for allowing us to conduct research at the old growth forest, which is in a Research Natural Area, and the Weyerhaeuser Company, for allowing us to conduct research at the mature and young sites.

## References

Anthoni, P. M., B. E. Law, and M. H. Unsworth (1999), Carbon and water vapor exchange of an open-canopied ponderosa pine ecosystem, *Agric. For. Meteorol.*, *95*, 151–168.

Anthoni, P. M., M. H. Unsworth, B. E. Law, J. Irvine, D. D. Baldocchi, S. Van Tuyl, and D. Moore (2002), Seasonal differences in carbon and water vapor exchange in young and old-growth ponderosa pine ecosystems, *Agric. For. Meteorol.*, *111*, 203–222.

Arain, M. A., T. A. Black, A. G. Barr, P. G. Jarvis, J. M. Massheder, D. L. Verseghy, and Z. Nesic (2002), Effects of seasonal and interannual climate variability on net ecosystem productivity of boreal deciduous and conifer forests, *Can. J. For. Res.*, *32*, 878–891.

Aubinet, M., B. Heinesch, and B. Longdoz (2002), Estimation of the carbon sequestration by a heterogeneous forest: Night flux corrections, heterogeneity of the site and inter-annual variability, *Global Change Biol.*, *8*, 1053–1071.

Barford, C. C., S. C. Wofsy, M. L. Goulden, J. W. Munger, E. H. Pyle, S. P. Urbanski, L. Hutyra, S. R. Saleska, D. Fitzjarrald, and K. Moore (2001), Factors controlling long- and short-term sequestration of atmospheric $CO_2$ in a mid-latitude forest, *Science*, *294*, 1688–1691.

Bowling, D. R., N. G. McDowell, J. M. Welker, B. J. Bond, B. E. Law, and J. R. Ehleringer (2003), Oxygen isotope content of $CO_2$ in nocturnal ecosystem respiration: 1. Observations in forests along a precipitation transect in Oregon, USA, *Global Biogeochem. Cycles*, *17*(4), 1120, doi:10.1029/2003GB002081.

Caspersen, J. P., S. W. Pacala, J. C. Jenkins, G. C. Hurtt, P. R. Moorcroft, and R. A. Birdsey (2000), Contributions of land-use history to carbon accumulation in U.S. forests, *Science*, *290*, 1148–1151.

Cohen, W. B., M. E. Harmon, D. O. Wallin, and M. Fiorella (1996), Two decades of carbon flux from forests of the Pacific Northwest, *Bioscience*, *46*, 836–844.

Easterling, D. R., G. A. Meehl, C. Parmesan, S. A. Changnon, T. R. Karl, and L. O. Mearns (2000), Climate extremes: Observations, modeling, and impacts, *Science*, *289*, 2068–2074.

Falge, E., et al. (2001), Gap filling strategies for defensible annual sums of net ecosystem exchange, *Agric. For. Meteorol.*, *107*, 43–69.

Farquhar, G. D., and S. von Caemmerer (1982), Modelling of photosynthetic response to the environment, in *Physiological Plant Ecology II: Encyclopedia of Plant Physiology*, edited by O. L. Lange et al., pp. 549–587, Springer-Verlag, New York.

Goldstein, A. H., N. E. Hultman, J. M. Fracheboud, M. R. Bauer, J. A. Panek, M. Xu, Y. Qi, A. B. Guenther, and W. Baugh (2000), Effects of climate variability on the carbon dioxide, water, and sensible heat fluxes above a ponderosa pine plantation in the Sierra Nevada (CA), *Agric. For. Meteorol.*, *101*, 113–129.

Goodale, C. L., et al. (2002), Forest carbon sinks in the Northern Hemisphere, *Ecol. Appls.*, *12*, 891–899.

Goulden, M. L., J. W. Munger, S. M. Fan, B. C. Daube, and S. C. Wofsy (1996), Measurements of carbon sequestration by long-term eddy covariance: Methods and a critical evaluation of accuracy, *Global Change Biol.*, *2*, 169–182.

Granier, A. (1987), Evaluation of transpiration in a Douglas-fir stand by means of sap flow measurements, *Tree Physiol.*, *3*, 309–320.

Griffis, T. J., T. A. Black, K. Morgenstern, A. G. Barr, Z. Nesic, G. B. Drewitt, D. Gaumont-Guay, and J. H. McCaughey (2003), Ecophysiological controls on the carbon balances of three southern boreal forests, *Agric. For. Meteorol.*, *117*, 53–71.

Hargrove, W. H., F. M. Hoffman, and B. E. Law (2003), New analysis reveals representativeness of the AmeriFlux network, *Eos Trans. AGU*, *84*, 529.

Irvine, J., and B. E. Law (2002), Contrasting soil respiration in young and old-growth ponderosa pine forests, *Global Change Biol.*, *8*, 1183–1194.

Irvine, J., B. E. Law, P. M. Anthoni, and F. C. Meinzer (2002), Water limitations to carbon exchange in old-growth and young ponderosa pine stands, *Tree Physiol.*, *22*, 189–196.

Irvine, J., B. E. Law, M. R. Kurpius, P. M. Anthoni, D. Moore, and P. A. Schwarz (2004), Age-related changes in ecosystem structure and function and effects on water and carbon exchange in ponderosa pine, *Tree Physiol.*, *24*, 753–763.

Janssens, I. A., et al. (2001), Productivity overshadows temperature in determining soil and ecosystem respiration across European forests, *Global Change Biol.*, *7*, 269–278.

Kelliher, F. M., D. J. Ross, B. E. Law, D. D. Baldocchi, and N. J. Rodda (2004), Limitations to carbon mineralization in litter and mineral soil of young and old ponderosa pine forests, *For. Ecol. Manage.*, *191*, 201–213.

Kramer, K., et al. (2002), Evaluation of six process-based forest growth models using eddy-covariance measurements of $CO_2$ and $H_2O$ fluxes at six forest sites in Europe, *Global Change Biol.*, *8*, 213–230.

Landsberg, J. J., and S. T. Gower (1997), *Applications of Physiological Ecology to Forest Management*, Academic, San Diego, Calif.

Law, B. E., D. D. Baldocchi, and P. M. Anthoni (1999a), Below-canopy and soil $CO_2$ fluxes in a ponderosa pine forest, *Agric. For. Meteorol.*, *94*, 171–188.

Law, B. E., M. G. Ryan, and P. M. Anthoni (1999b), Seasonal and annual respiration of a ponderosa pine ecosystem, *Global Change Biol.*, *5*, 169–182.

Law, B. E., M. Williams, P. M. Anthoni, D. D. Baldocchi, and M. H. Unsworth (2000), Measuring and modelling seasonal variation of carbon dioxide and water vapour exchange of a Pinus ponderosa forest subject to soil water deficit, *Global Change Biol.*, *6*, 613–630.

Law, B. E., A. Cescatti, and D. D. Baldocchi (2001a), Leaf area distribution and radiative transfer in open-canopy forests: Implications for mass and energy exchange, *Tree Physiol.*, *21*, 777–787.

Law, B. E., F. M. Kelliher, D. D. Baldocchi, P. M. Anthoni, J. Irvine, D. Moore, and S. Van Tuyl (2001b), Spatial and temporal variation in respiration in a young ponderosa pine forests during a summer drought, *Agric. For. Meteorol.*, *110*, 27–43.

Law, B. E., P. E. Thornton, J. Irvine, P. M. Anthoni, and S. Van Tuyl (2001c), Carbon storage and fluxes in ponderosa pine forests at different developmental stages, *Global Change Biol.*, *7*, 755–777.

Law, B. E., O. J. Sun, J. Campbell, S. Van Tuyl, and P. E. Thornton (2003), Changes in carbon storage and fluxes in a chronosequence of ponderosa pine, *Global Change Biol.*, *9*, 510–524.

Law, B. E., D. P. Turner, M. A. Lefsky, J. Campbell, M. Guzy, O. Sun, S. Van Tuyl, and W. B. Cohen (2004), Carbon fluxes across regions: Observational constraints at multiple scales, in *Scaling and Uncertainty Analysis in Ecology: Methods and Applications*, edited by J. Wu et al., Columbia Univ. Press, New York, in press.

Meiresonne, L., D. A. Sampson, A. S. Kowalski, I. A. Janssens, N. Nadezhdina, J. Cermak, J. Van Slycken, and R. Ceulemans (2003), Water flux estimates from a Belgian Scots pine stand: A comparison of different approaches, *J. Hydrol.*, *270*, 230–252.

Meyer, W. H. (1938), Yield of even-aged stands of ponderosa pine, *Tech. Bull. 630*, U.S. Dep. of Agric., Washington, D. C.

Moncrieff, J. B., Y. Malhi, and R. Leuning (1996), The propagation of errors in long-term measurements of land-atmosphere fluxes of carbon and water, *Global Change Biol.*, *2*, 231–240.

Myneni, R. B., J. Dong, C. J. Tucker, R. K. Kaufmann, P. E. Kauppi, J. Liski, L. Zhou, V. Alexeyev, and M. K. Hughes (2001), A large carbon sink in the woody biomass of Northern forests, *Proc. Natl. Acad. Sci. U. S. A.*, *98*, 14,784–14,789.

Oliver, W. W., and R. A. Ryker (1990), *Pinus ponderosa* Dougl. ex Laws. Ponderosa pine, in *Silvics of North America*, vol. 1, *Conifers*, *Agric. Handb.*, vol. 654, edited by R. M. Burns and B. H. Honkala, pp. 413–424, U.S. Dep. of Agric., Washington, D. C.

Ryan, M. G. (2002), Canopy processes research, *Tree Physiol*, *22*, 1035–1043.

Ryan, M. G., and B. J. Yoder (1997), Hydraulic limits to tree height and tree growth, *Bioscience*, *47*, 235–242.

Ryan, M. G., D. Binkley, J. H. Fownes, C. P. Giardina, and R. S. Senock (2004), An experimental test of the causes of forest growth decline with stand age, *Ecol. Monogr.*, *74*, 393–414.

Schaefer, K., A. S. Denning, N. Suits, J. Kaduk, I. Baker, S. Los, and L. Prihodko (2002), Effect of climate on interannual variability of terrestrial $CO_2$ fluxes, *Global Biogeochem. Cycles*, *16*(4), 1102, doi:10.1029/2002GB001928.

Schimel, D., et al. (2000), Contribution of increasing $CO_2$ and climate to carbon storage by ecosystems in the United States, *Science*, *287*, 2004–2006.

Schimel, D. S., et al. (2001), Recent patterns and mechanisms of carbon exchange by terrestrial ecosystems, *Nature*, *414*, 169–172.

Stone, E. L., and P. J. Kalisz (1991), On the maximum extent of tree roots, *For. Ecol. Manage.*, *46*, 59–102.

Sun, O. J., J. L. Campbell, and B. E. Law (2004), Dynamics of carbon storage in soils and detritus across chronosequences of different forest types in the Pacific Northwest, USA, *Global Change Biol.*, in press.

Suni, T., F. Berninger, T. Markkanen, P. Keronen, U. Rannik, and T. Vesala (2003), Interannual variability and timing of growing-season $CO_2$ exchange in a boreal forest, *J. Geophys. Res.*, *108*(D9), 4265, doi:10.1029/2002JD002381.

Turner, D. P., G. J. Koerper, M. E. Harmon, and J. L. Lee (1995), A carbon budget for forests on the conterminous United States, *Ecol. Appl.*, *5*, 421–436.

Valentini, R., et al. (2000), Respiration as the main determinant of carbon balance in European forests, *Nature*, *404*, 861–865.

Valentini, R., G. Matteucci, A. J. Dolman, and E. D. Schulze (2003), Conclusions: The role of canopy flux measurements in global C-cycle research, in *Fluxes of Carbon, Water, and Energy of European Forests*, edited by R. Valentini, pp. 255–266, Springer-Verlag, New York.

Wallach, D., and B. Goffinet (1987), Mean squared error of prediction in models for studying ecological and agronomic system, *Biometrics*, *43*, 561–573.

Wallach, D., and B. Goffinet (1989), Mean squared error of prediction as a criterion for evaluating and comparing system models., *Ecol. Modell.*, *4*, 299–306.

Wang, K. Y., S. Kellomaki, T. S. Zha, and H. Peltola (2004), Component carbon fluxes and their contribution to ecosystem carbon exchange in a pine forest: An assessment based on eddy covariance measurements and an integrated model, *Tree Physiol.*, *24*, 19–24.

Waring, R. H., and S. W. Running (1978), Sapwood water storage: Its contribution to transpiration and effect upon water conductance through stems of old-growth Douglas-fir, *Plant Cell Environ.*, *1*, 131–140.

Weltzin, J. F., et al. (2003), Assessing the response of terrestrial ecosystems to potential changes in precipitation, *Bioscience*, *53*, 941–952.

Williams, M., E. B. Rastetter, D. N. Fernandes, M. L. Goulden, S. C. Wofsy, G. R. Shaver, J. M. Melillo, J. W. Munger, S. M. Fan, and K. J. Nadelhoffer (1996), Modelling the soil-plant-atmosphere continuum in a Quercus-Acer stand at Harvard forest: The regulation of stomatal conductance by light, nitrogen and soil/plant hydraulic properties, *Plant Cell Environ.*, *19*, 911–927.

Williams, M., Y. Malhi, A. D. Nobre, E. B. Rastetter, J. Grace, and M. G. P. Pereira (1998), Seasonal variation in net carbon exchange and evapotranspiration in a Brazilian rain forest: A modelling analysis, *Plant Cell Environ.*, *21*, 953–968.

Williams, M., W. Eugster, E. B. Rastetter, J. P. McFadden, and F. S. Chapin (2000), The controls on net ecosystem productivity along an Arctic transect: A model comparison with flux measurements, *Global Change Biol.*, *6*, 116–126.

Williams, M., B. J. Bond, and M. G. Ryan (2001a), Evaluating different soil and plant hydraulic constraints on tree function using a model and sap flow data from ponderosa pine, *Plant Cell Environ.*, *24*, 679–690.

Williams, M., B. E. Law, P. M. Anthoni, and M. H. Unsworth (2001b), Use of a simulation model and ecosystem flux data to examine carbon-water interactions in ponderosa pine, *Tree Physiol.*, *21*, 287–298.

Wilson, K. B., P. J. Hanson, P. J. Mulholland, D. D. Baldocchi, and S. D. Wullschleger (2001), A comparison of methods for determining forest evapotranspiration and its components: Sap-flow, soil water budget, eddy covariance and catchment water balance, *Agric. For. Meteorol.*, *106*, 153–168.

Xu, L., and D. D. Baldocchi (2004), Seasonal variation in carbon dioxide exchange over a Mediterranean annual grassland in California, *Agric. For. Meteorol.*, *123*, 79–96.

Yoder, B. J., M. G. Ryan, R. H. Waring, A. W. Schoettle, and M. R. Kaufmann (1994), Evidence of reduced photosynthetic rates in old trees, *For. Sci.*, *40*, 513–527.

Zimmermann, M. H. (1983), *Xylem Structure and the Ascent of Sap*, Springer-Verlag, New York.

J. Irvine, B. E. Law, D. Moore, and P. A. Schwarz, College of Forestry, Oregon State University, Corvallis, OR 97331-5752, USA. (paul.schwarz@oregonstate.edu)

M. Kurpius, College of Oceanic and Atmospheric Sciences, Oregon State University, Corvallis, OR 97331-5503, USA.

M. Williams, School of GeoSciences, University of Edinburgh, Darwin Building, Kings Buildings, Mayfield Road, Edinburgh EH9 3JU, UK.